Aspheric silicon lenses for terahertz photoconductive antennas

Florian Formanek,[a] Marc-Aurèle Brun, Tomoyuki Umetsu, Shinji Omori, and Akio Yasuda
Life Science Laboratory, Materials Laboratories, Sony Corporation, Sony Bioinformatics Center, Tokyo Medical and Dental University, 1-5-45 Yushima, Bunkyo-ku, Tokyo 113-8510, Japan

(Received 27 October 2008; accepted 23 December 2008; published online 14 January 2009)

We report on the design and characterization of aspheric focusing silicon lenses for terahertz photoconductive antennas. The lenses are engineered using ray-tracing software and characterized using an optical fiber terahertz time-domain spectroscopy system. We find that using aspheric lenses improves terahertz radiation coupling from the emitter and enables improved collection by the detector. The signal-to-noise ratio and the cutoff frequency of measured terahertz spectra are improved. Minimized aberrations also reduce the focal spot size. Simulations based on Fresnel–Kirchhoff diffraction theory, taking into account the radiation pattern of the emitter and aberrations of the lenses, show good agreement with our measurements. © *2009 American Institute of Physics*. [DOI: 10.1063/1.3072357]

Since the pioneering work on photoconductive antennas to generate and detect broadband terahertz pulses,[1] terahertz time-domain spectroscopy (TDS) has become a powerful technique to study the properties of a wide range of materials in the far-infrared region. An important breakthrough, leading to the establishment of the technology, was the use of substrate lenses to allow free-space propagation of the terahertz pulses.[2] If there is no lens attached to the back of an antenna, most of the generated radiation remains trapped in the antenna substrate because of total internal reflection. Most TDS imaging experiments are performed with collimating lenses in combination with off-axis parabolic mirrors to focus the terahertz radiation. However, there is a clear advantage in using focusing lenses to produce compact terahertz TDS imaging systems.[3]

In this paper, we investigate focusing silicon lenses having an aspheric design, with the objective of improving the efficiency of terahertz beam recombination at the detector and improving the lateral resolution of the system in the focal plane by minimizing aberrations. A ray-tracing simulation is employed from an engineering point of view to assess the benefits of using such lenses. Experimental measurements are later described through calculations based on Fresnel–Kirchhoff diffraction theory.

Based on geometrical optics, it is possible to design a hyperhemispherical silicon lens that can focus light at a given distance from its apex.[4,5] For these experiments, we consider a lens with a radius $R=6.75$ mm and a focal length $f'=25$ mm (Fig. 1). Dipole-type photoconductive antennas made of gallium arsenide (GaAs) are used. The antennas have H-shaped gold electrodes with a 6 μm gap on 350 μm thick GaAs substrates. Ignoring the small discontinuity in refractive indices between silicon ($n=3.44$) and GaAs ($n=3.61$), the focal length is defined within the paraxial approximation by $1/f'=(n-1)/R-n/f$, where f is the distance from the lens apex to the emitter point source, $f=10.7$ mm in this case, and n is the refractive index of silicon. The offset is defined as the extension of the lens beyond hemisphericity and is equal to 3.6 mm. The critical emission angle θ_{tir} above which radiation remains trapped inside the lens because of total internal reflection is 30.3° for this spherical lens.

The aspheric lenses are designed with the software CODE V (Optical Research Associates) to minimize aberrations according to the equation

$$z=\frac{ch^2}{1+\sqrt{1-c^2h^2}}+Ah^4+Bh^6+Ch^8+Dh^{10}, \tag{1}$$

where $c=1/R$ is the curvature and h is the height from the optical axis. A, B, C, and D represent the fourth, sixth, eighth, and tenth order aspheric coefficients, respectively. In our design $A=-1.126\times10^{-4}$, $B=-3.874\times10^{-6}$, $C=1.094\times10^{-7}$, and $D=-4.274\times10^{-9}$. By allowing radiation emitted at larger angles with respect to the optical axis to be coupled out of the lens, the aspheric design increases the strength of the detected signals as well as the numerical aperture of the system. The critical emission angle θ_{tir} becomes 38.9°. Due to the close dielectric interfaces, the radiation pattern from the emitter differs from that of a free-space dipole and shows a particular angular distribution.[6] For the ray-tracing simulation, the illuminance is weighted gradually, as shown in Fig. 1. The emitter is considered to be a 6 μm diameter circular source.

Calculated illuminance profiles at the focal plane are shown in Fig. 2. The efficiency of the radiation transmission from the emitter to a 2×2 mm^2 surface in the focal plane is estimated to 1.65% and 11.79% for spherical and aspheric lenses. The double-peak shape visible in the aspheric case is due to the nonuniform radiation pattern of the emitter, which can be represented by an annular source. Due to aberrations

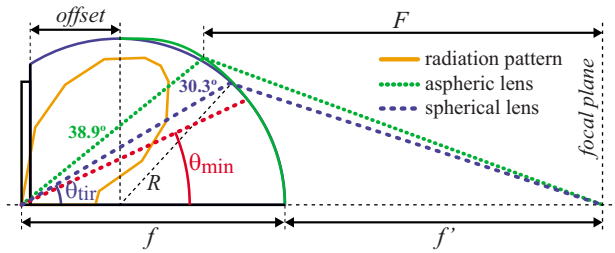

FIG. 1. (Color online) Schematic view of half of a focusing silicon lens. Rays at maximum emission angles corresponding to the total internal reflection limit are traced.

[a]Electronic mail: florian.formanek@jp.sony.com.

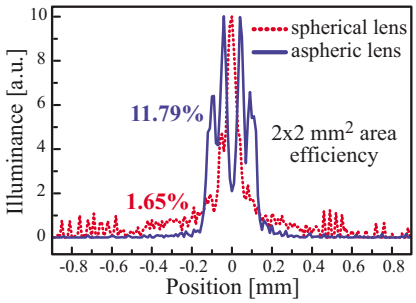

FIG. 2. (Color online) Normalized illuminance profiles at the focal plane, centered around the optical axis, obtained by ray-tracing simulations.

in the spherical case, the light wavefront is deformed along the optical axis. Thus, the image of the radiation pattern in the focal plane is blurred and the illuminance profile appears as a single peak. For comparison, 80% of the illuminance is included in 1.54×1.54 and 0.38×0.38 mm^2 areas for the spherical and aspheric cases. The total efficiency of the radiation transmission from the emitter to a 50×50 μm^2 surface in the detector plane is estimated to be 0.11% and 5.7% for spherical and aspheric lenses. This corresponds to a ~52 times increase.

The characteristics of the aspheric lenses were experimentally compared with those of the spherical lenses using a terahertz TDS system based on a Ti:Sapphire laser delivering 80 fs pulses at 780 nm. The laser beam is split into a pump and a probe beam, the latter being optically delayed with a retroreflector mounted on a computer-controlled translation stage. Our system uses optical fibers for the delivery of the excitation pulses. The group velocity dispersion introduced by the fibers is precompensated by a grating pair. A fiber system has the advantage of avoiding the need for realignment between the optical probe beam and the antenna when moving the detector. The optical powers sent on the emitter and detector are 8 mW each. The electrodes of the emitter are biased with a square voltage of −5 to 5 V modulated at 40 kHz. The current at the detector electrodes is measured with a lock-in amplifier. The aspheric lenses are polished from bare high-resistivity silicon blocks. The emitter and detector are attached to two focusing lenses, either the aspheric lenses or the spherical lenses. The emitter is fixed while the detector is mounted on an *XYZ* translation stage with micrometer resolution for precise positioning. The lenses are placed at a distance twice their focal length from each other.

Figure 3(a) shows the recorded time-domain spectra. The maximum current measured at the detector electrodes is ~4.6 times higher when using the aspheric lenses. The time-domain signal-to-noise ratio in amplitude is ~60 dB with

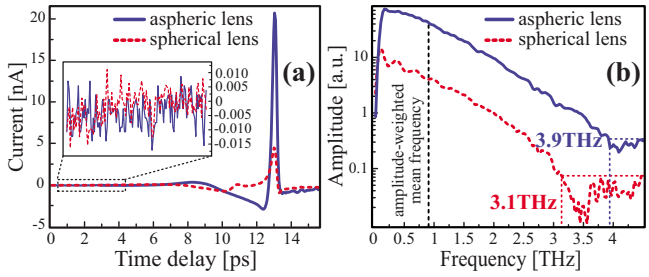

FIG. 3. (Color online) (a) Time-domain spectra recorded using the spherical and aspheric focusing lenses. (b) Corresponding amplitude spectra obtained after Fourier transform.

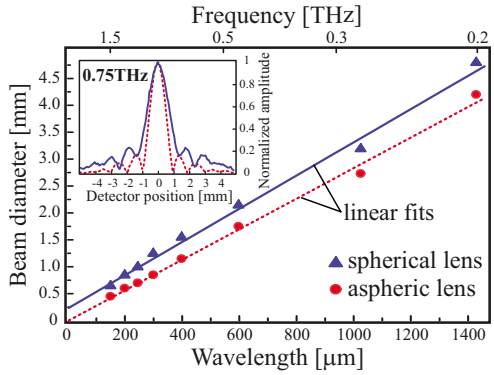

FIG. 4. (Color online) Experimentally determined terahertz beam diameter at discrete frequencies from 0.2 to 1.5 THz for the spherical and aspheric lenses. Inset: amplitude profiles.

the aspheric lenses and ~48 dB with the spherical lenses. Figure 3(b) shows the corresponding amplitude spectra obtained after Fourier transform. The improvement in the frequency bandwidth when using aspheric lenses is clear; as the cutoff frequency increases from 3.1 to 3.9 THz. This can be explained by the fact that more radiation is able to exit the aspheric lens. The ratio of the amplitudes measured at the amplitude-weighted mean frequency (~0.85 THz) is close to 10. In comparison, ray-tracing simulations predicted an amplitude ratio of 7.2.

To evaluate the terahertz beam size in the focal plane with high spatial resolution, the detector was used without a silicon lens. A time-domain spectrum was recorded for each position of the detector in the plane perpendicular to the axis of the antenna dipole. Amplitude profiles for discrete frequencies were obtained after Fourier transform, as shown in the inset of Fig. 4. These frequency-dependent profiles were fitted with Gaussian functions and their full widths at half maximum were determined. The results are shown in Fig. 4 as a function of the wavelength and fitted by a linear regression. A maximum improvement in resolution of 600 μm is seen for longer wavelengths (~1430 μm). At 2 THz, the beam diameter is as small as 450 μm when using aspheric lenses and 200 μm smaller than with spherical lenses. The nonzero value at the origin of the linear fit for the spherical lens data reveals the resolution limitation imposed by spherical aberrations.

Our results can be understood by considering the diffraction of the terahertz beam by the finite aperture defined by the silicon lens. The system is equivalent to a single focusing lens with a circular aperture. The Fresnel–Kirchhoff diffraction theory[7] can be applied to calculate the frequency-dependent electric field in the focal plane of this lens. We also take into account the radiation pattern of the emitter within the silicon lens[8,9] and consider that terahertz emission occurs uniformly between two angles θ_{tir} and θ_{min}. The angle θ_{tir} corresponds to the angle for total internal reflection at the silicon-air interface, while θ_{min} is defined arbitrarily as the angle for which the radiation pattern reaches 80% of its maximum value. For the spherical lens, we have $\theta_{tir}=30.3°$ and $\theta_{min}=25°$. For the aspheric lens, we have $\theta_{tir}=38.9°$. Therefore, the diffracting silicon lens can be represented by an annular aperture with outer and inner diameters D_{tir} and D_{min} defined by the angles θ_{tir}, θ_{min}, and the shape of the lenses. Ray-tracing simulations show that the effect of aberrations on the terahertz beam shape at the focus can be im-

portant. For this reason we also consider the wavefront aberrations of the terahertz beam due to the silicon lens. Noting the rotational symmetry of the system around the optical axis, the electric field distribution in the focal plane is given in polar coordinates by[10]

$$E(r,\lambda) \propto \left| \int_{\varepsilon}^{1} \int_{0}^{2\pi} \wp(\rho) J_0[(\pi D_{\mathrm{tir}} r/\lambda F)\rho] \rho d\rho d\theta \right|, \qquad (2)$$

where λ is the radiation wavelength, r is the radial distance from the optical axis, J_0 is the zero-order Bessel function, $\varepsilon = D_{\mathrm{min}}/D_{\mathrm{tir}}$, and F is the effective focal length from the position defined by the total internal reflection angle. The radial coordinate ρ is normalized to be equal to 1 at the edge of the aperture. The pupil function of the aperture $\wp(\rho)$ accounts for the aberrations of the lens. Considering only spherical aberrations and astigmatism, the pupil function can be expressed as

$$\wp(\rho) = \exp\left[i \frac{2\pi}{\lambda} (W_{040}\rho^4 + W_{222} r^2 \rho^2 \cos^2 \theta) \right], \qquad (3)$$

where W_{040} and W_{222} are the spherical and astigmatism aberration coefficients, respectively.

The solid lines in Fig. 5 show the results of the calculation using the annular aperture and taking into account the aberrations. The simulations show good agreement with the experimental data, up to the second minima of the amplitude profiles. However, if the aberrations of the spherical lens are not considered, see the dashed curves in Figs. 5(a)–5(c), the calculated profiles differ from the theoretical profiles. Especially, the nonzero value of the lowest frequency minimum is not reproduced. The dashed curves in Figs. 5(d)–5(f) were obtained by considering the aspheric silicon lenses as circular apertures with D_{tir} diameters rather than annular apertures ($\varepsilon = 0$), i.e., by neglecting the effect of the radiation pattern of the emitter. In this case, the calculated profiles clearly appear broader and cannot account for the experimental data.

In conclusion, we have shown the advantage of using focusing aspheric silicon lenses for terahertz TDS imaging systems. The improved radiation coupling from the emitter and the improved collection of radiation by the detector increase the signal-to-noise ratio by roughly 12 dB. The cutoff frequency was increased from 3.1 to 3.9 THz, and the diameter of the terahertz beam in the focal plane was reduced. Simulations based on Fresnel–Kirchhoff diffraction theory confirmed the importance of considering the aberrations and the radiation pattern of the emitter in designing the silicon lenses attached to terahertz photoconductive antennas. A gain in efficiency for the more common collimating type lenses is also expected since the critical emission angle would also be increased.

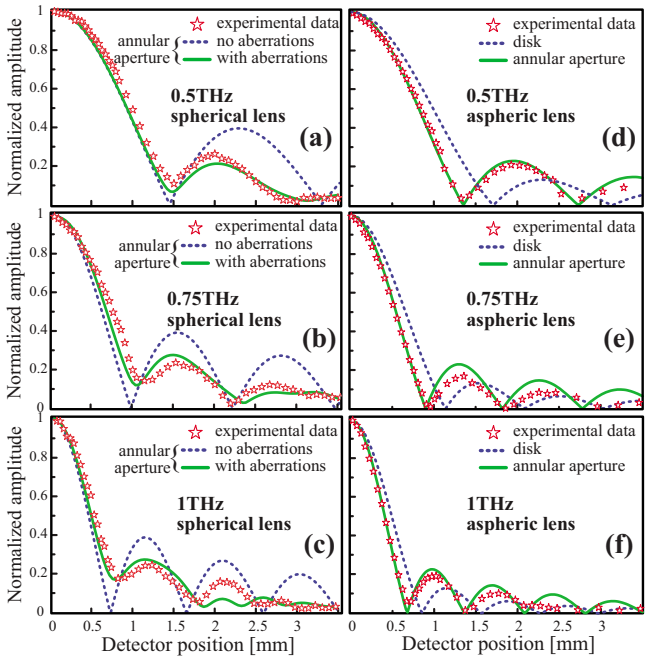

FIG. 5. (Color online) Amplitude profiles at the focal plane measured experimentally and compared with Fresnel–Kirchhoff diffraction theory.

[1] D. H. Auston, K. P. Cheung, and P. R. Smith, Appl. Phys. Lett. **45**, 284 (1984).
[2] C. Fattinger and D. Grischkowsky, Appl. Phys. Lett. **54**, 490 (1989).
[3] B. B. Hu and M. C. Nuss, Opt. Lett. **20**, 1716 (1995).
[4] R. Inoue, Y. Ohno, and M. Tonouchi, Jpn. J. Appl. Phys., Part 1 **45**, 7928 (2006).
[5] J. Van Rudd and D. M. Mittleman, J. Opt. Soc. Am. B **19**, 319 (2002).
[6] W. Lukosz, J. Opt. Soc. Am. **69**, 1495 (1979).
[7] M. Born and E. Wolf, *Principles of Optics*, 7th ed. (Cambridge University Press, Cambridge, 1999).
[8] P. U. Jepsen and S. R. Keiding, Opt. Lett. **20**, 807 (1995).
[9] M. T. Reiten and R. A. Cheville, Opt. Lett. **30**, 673 (2005).
[10] J. C. Wyant and K. Creath, in *Applied Optics and Optical Engineering*, edited by J. C. Wyant and R. R. Shannon (Academic, New York, 1992), pp. 2–53.